Published in final edited form as:
*J Comp Neurol*. 2004 August 2; 475(4): 463–480. doi:10.1002/cne.20170.

# Expression of Calcium Transporters in the Retina of the Tiger Salamander (Ambystoma tigrinum)

**DAVID KRIŽAJ**[1,2,*], **XIAORONG LIU**[1], and **DAVID R. COPENHAGEN**[1,2]

1*Department of Ophthalmology, University of California, San Francisco, School of Medicine, San Francisco, California 94143-0730*

2*Department of Physiology, University of California, San Francisco, School of Medicine, San Francisco, California 94143-0730*

## Abstract

Changes in intracellular calcium concentration, $[Ca^{2+}]i$, modulate the flow of visual signals across all stages of processing in the retina, yet the identities of $Ca^{2+}$ transporters responsible for these changes are still largely unknown. In the current study, the distribution of plasma membrane and intracellular $Ca^{2+}$ transporters in the retina of tiger salamander, a model system for physiological studies of retinal function, was determined. Plasma membrane calcium ATPases (PMCAs), responsible for high-affinity $Ca^{2+}$ extrusion, were highly expressed in the salamander retina. PMCA isoforms 1, 2, and 4 were localized to photoreceptors, whereas the inner retina expressed all four isoforms. PMCA3 was expressed in a sparse population of amacrine and ganglion neurons, whereas PMCA2 was expressed in most amacrine and ganglion cells. $Na^{+}/Ca^{2+}$ exchangers, a high-capacity $Ca^{2+}$ extrusion system, were expressed in the outer plexiform layer and in a subset of inner nuclear and ganglion layer cells. Intracellular $Ca^{2+}$ store transporters were also represented prominently. SERCA2a, a splice variant of the sarcoplasmic-endoplasmic $Ca^{2+}$ ATPase, was found mostly in photoreceptors, whereas SERCA2b was found in the majority of retinal neurons and in glial cells. The predominant endoplasmic reticulum (ER) $Ca^{2+}$ channels in the salamander retina are represented by the isoform 2 of the $IP_3$ receptor family and the isoform 2 of the ryanodine receptor family. These results indicate that $Ca^{2+}$ transporters in the salamander retina are expressed in a cell type-specific manner.

### Keywords

PMCA; SERCA; ryanodine receptor; photoreceptor; Na/Ca exchanger; amacrine cell

Calcium ion is a universal intracellular messenger that regulates an elaborate network of intracellular signaling pathways. Because $Ca^{2+}$-regulated pathways can distinguish between calcium signals of differing properties, $Ca^{2+}$ can control a variety of different functions in different parts of the cell (Delmas and Brown, 2003). The amplitude of the $Ca^{2+}$ signal, the temporal and spatial pattern of $Ca^{2+}$ entry, buffering, and extrusion are all parameters critical for specificity of cell responses (Berridge et al., 2003). To understand $Ca^{2+}$ signaling, it is therefore important to map the distribution of $Ca^{2+}$ effector proteins, such as $Ca^{2+}$ channels, $Ca^{2+}$ pumps, cytoplasmic buffers, and intracellular $Ca^{2+}$ stores.

*Correspondence to: David Križaj, Dept. Ophthalmology, Beckman Vision Center, Rm. K-140, UCSF School of Medicine, 10 Kirkham St., San Francisco, CA 94143-0730. E-mail: krizaj@phy.ucsf.edu

In retina, dynamic changes in intracellular calcium concentration, $[Ca^{2+}]i$, control both transduction and transmission of the visual signal across retinal pathways (reviewed in Fain et al., 2001; Akopian and Witkovsky, 2002). Cellular functions under control of $Ca^{2+}$ include regulation of gene expression, membrane excitability, synaptic transmission, and light adaptation (Fain et al., 2001; Križaj and Copenhagen, 2002). Stimulus-evoked $[Ca^{2+}]i$ changes in retinal neurons can be transient, sustained, or oscillatory, depending on concerted action of plasma membrane voltage-gated $Ca^{2+}$ channels and $Ca^{2+}$ pumps as well as intracellular $Ca^{2+}$ release and sequestration mechanisms (Euler et al., 2002; Hurtado et al., 2002; Lohmann et al., 2002; Križaj et al., 2003). Accumulated evidence increasingly points to $Ca^{2+}$ release from the endoplasmic reticulum (ER) as having a key role in many aspects of retinal $Ca^{2+}$ homeostasis. $Ca^{2+}$ release from internal stores regulates $[Ca^{2+}]i$ in photoreceptors (Križaj et al., 2003), horizontal cells (Micci and Christensen, 1998; Solessio and Lasater, 2002), amacrine cells (Hurtado et al., 2002; Sosa et al., 2003), ganglion cells (Akopian and Witkovsky, 2001, 2002), as well as in Müller glia (Keirstead and Miller, 1995; Newman 2001), and plays a role in development of the retina (Sugioka et al., 1998; Lohmann et al., 2002) and synaptic signaling (Križaj et al., 1999). At present, little is known about the localization of ER $Ca^{2+}$ transport systems within the retina, nor have the specific isoforms of ryanodine receptors, $IP_3$ receptors, NCXs, and SERCA pumps been identified for any vertebrate retina.

The amphibian retina in general, and that of the tiger salamander (*Ambystoma tigrinum*) in particular, have become a model system for physiological investigations of retinal function, mainly due to the large size of salamander retinal cells and excellent survival of retinal slices and dissociated cells. Following the pioneering studies in the mudpuppy (*Necturus maculosus*) by Werblin and Dowling (1969), tiger salamander retinal neurons have been studied using intracellular ion indicator imaging (Wellis and Werblin, 1995; Križaj and Copenhagen, 1998), electrophysiological (Capovilla et al., 1987; Lukasiewicz and Werblin, 1990; Wu, 1991; Lamb and Pugh, 1992), electron microscopical (Lasansky, 1973; Townes-Anderson et al., 1985), immunohistochemical (Deng et al., 2001; Sherry et al., 2001), and multielectrode array (Meister et al., 1995) techniques. Many investigations into the role of $Ca^{2+}$-dependent processes in visual signaling have provided fundamental insights into retinal function. The majority of these studies focused on the mechanisms of $Ca^{2+}$ influx into salamander retinal cells. The aim of this study was to characterize the mechanisms that control cytoplasmic free $[Ca^{2+}]$ in neurons from the salamander retina by extruding it from the cytoplasm into extracellular space and by sequestering and releasing $Ca^{2+}$ from intracellular stores. We mapped the distribution and cellular localization of transporters responsible for $Ca^{2+}$ extrusion across the plasma membrane (such as the various isoforms and splice variants of the plasma membrane $Ca^{2+}$ ATPase (PMCA) family and the sodium-calcium exchanger (NCX)), sarcoplasmic-endoplasmic $Ca^{2+}$ ATPase (SERCA) pumps responsible for $Ca^{2+}$ sequestration into intracellular $Ca^{2+}$ stores, ryanodine (RyR), and $IP_3$ receptors ($IP_3R$). This is, to the best of our knowledge, the first comprehensive effort to identify $Ca^{2+}$ transporters in a vertebrate retina.

## MATERIALS AND METHODS

### Animals and tissue preparation

Retinas of neotenic tiger salamanders (*Ambystoma tigrinum*) were investigated (Sullivan, Nashville, TN). The animals were killed by decapitation and pithing. The eyes were enucleated, corneas were cut with a razor blade, and the eyecups with the retinas were immersion-fixed for one-half to one hour in 4% (w/v) paraformaldehyde in phosphate buffer (PB; 0.1M; pH 7.4). The retinas were rinsed two times in PBS and cryoprotected in 30% sucrose overnight at 4°C. Pieces of retinas were mounted in OCT, sectioned vertically at 14 μm thickness on a

cryostat, collected on Super-Frost Plus slides (Fisher, Pittsburgh, PA), and stored at -20°C until use.

## Immunohistochemistry

Antibodies used in our experiments are listed in Table 1. The isoform-specific anti-PMCA antibodies were a generous gift from Drs. John T. Penniston and Emanuel E. Strehler (Mayo Clinic, Rochester, MN) or obtained commercially from Swiss Antibodies (Swant, Bellinzona, Switzerland) and Affinity Bioreagents (ABR, Golden, CO). Rabbit polyclonal antibodies NR1, NR2, and NR3 against PMCA 1, 2, and 3, respectively, were generated against 13–18 residue peptide sequences at the amino terminus of the corresponding rat PMCA (Filoteo et al., 1997), whereas mouse monoclonal antibody JA9 was raised against human erythrocyte PMCA and recognizes a sequence close to the N-terminus of PMCA4. The specificity of all PMCA antibodies has been fully characterized by Western blots of COS cell microsomes containing overexpressed PMCAs of known identity (Filoteo et al., 1997). The Swant antibodies were generated in rabbit against an N-terminal sequence of the human PMCA1-4 (Stauffer et al., 1995). SERCA1, RyR1, and SV2 antibodies (developed by Judith Airey, John Sutko, and Kathleen Buckley, respectively) were obtained from the Developmental Studies Hybridoma Bank; SERCA 2a and 2b antibodies were a generous gift from Prof. Frank Wuytack from Katholieke Universiteit in Leiden; the SERCA3 antibody was purchased from Sigma (St. Louis, MO) or ABR; tyrosine hydroxylase antibody from Chemicon (Temecula, CA), and the $IP_3R3$ antibody from Transduction Labs (San Diego, CA). All immunostaining was done with controls incubated in secondary antibodies alone. In addition, because of weak immunofluorescence (SERCA3) or lack of reactivity with the Western blotting procedure ($IP_3R2$), we performed competitive binding studies in which equal amounts of primary antibody and its specific neutralizing peptide were co-incubated during the first step of the procedure (see below). The $IP_3R2$ neutralizing peptide (PA1-904; ABR) was derived from the cytoplasmic, NH3terminal domain of rat $IP_3R2$; the SERCA3 neutralizing peptide was a synthetic peptide of 11 amino acid from a conserved sequence of the $NH_3$-terminal domain of the SERCA3 protein (PA-910, ABR).

The retinal sections were washed in PBS for 15 minutes, then permeabilized and blocked in a solution containing 0.5% Triton X-100 and 10% goat serum. The sections were incubated with primary antibodies overnight at 4°C. For double-labeling experiments, a mixture of primary antibodies was applied followed by a mixture of secondary antibodies. After three 5-minute washes in PBS, secondary antibodies were applied for 2 hours. The following secondary antibodies were utilized: Alexa 488 and Alexa 594 nm goat antimouse, goat antirat, or goat antirabbit IgG ($H^+L$) conjugates (Molecular Probes, Eugene, OR), diluted 1:1,000. After incubation, sections were washed in PB for 30 minutes and mounted with Vectashield (Vector, Burlingame, CA). Negative controls were performed for every set of experiments by omitting the primary antibody.

## Western blots

Although all antibodies used in our experiments were characterized and utilized in immunohistochemistry on mammalian preparations, only a few have been characterized in amphibian preparations (RyR2, Lai et al., 1992; NR1-PMCA1, NR2-PMCA2, NR3-PMCA3, and JA9-PMCA4, Dumont et al., 2001; 5F10, Yamoah et al., 1998). To determine whether antibodies used in our experiments recognized epitopes from amphibian preparations, we performed Western blots with salamander retinal tissues (Fig. 1). Since most of the antibodies were raised against mammalian epitopes, Western blots with mouse retinae were simultaneously performed.

Cytoplasmic and nuclear proteins were prepared using the NE-PER extraction reagents (Pierce Biotechnology, Rockford, IL). The protein concentrations were determined by BCA protein Assay Kit (Pierce Biotechnology). Equal amounts of protein lysate were loaded from total salamander and mouse retinas. 15–25 μg of extract were resolved on NOVEX-NuPAGE 4 – 12% BT gels (Invitrogen, La Jolla, CA), and transferred to PVDF membranes (Invitrogen). After blocking with 5% nonfat milk in washing buffer (1× PBS+ 0.1% Tween-20), the membranes were incubated with primary isoform-specific antibodies at 4°C overnight. After washing, the blots were then incubated with appropriate antiperoxidase-conjugated secondary antibodies (1:4,000, Amersham Life Sciences, Arlington Heights, IL) at room temperature for 2–3 hours. Finally, the proteins on the membranes were detected using the ECL+plus chemiluminescence system (Amersham Pharmacia Biotech).

### Image acquisition and processing

Immunofluorescent and bright-field Nomarski fields of view were obtained using a confocal microscope (Zeiss LSM 5 Pascal) at 2% power for the 488 nm argon line and 100% power for the helium-neon line. During acquisition of signals from double-labeled sections, the scans were collected sequentially to prevent spectral bleed-through. Acquired images were processed with Adobe Photoshop (v. 7.0; San Jose, CA) software.

## RESULTS

We first determined the location of several transport systems in the ER, including SERCA pumps, RyRs, and $IP_3$Rs. We then turned to analyze the distribution of $Ca^{2+}$ ATPases and the $Na+/Ca^{2+}$ exchangers in the plasma membrane of retinal cells.

Western blots revealed that SERCA 2 and 3 isoforms and the $Na+/Ca^{2+}$ exchanger (NCX) are expressed in both salamander and mouse retina (Fig. 1; the distribution of SERCA isoforms in the mouse retina will be analyzed in detail in another publication: D.K., in prep.). In both species bands were detected at kDa ranges close to the expected molecular weights (MW). The SERCA2 band positions in mouse and salamander were close to the expected 110 kDa MW band, whereas the SERCA3 signal was at the expected 97 kDa band (Wuytack et al., 1989, 2002). The SERCA2b doublet in mouse may show a contribution from another SERCA2 splice variant (e.g., Martin et al., 2002). The NCX band in salamander was close to the 120 kDa position corresponding to a full length exchanger. The dominant NCX signal was slightly lower than in mouse, possibly because salamander expresses a different splice variant (Wei et al., 2003). Although PMCA antibodies used in our studies were characterized extensively in another amphibian preparation (Dumont et al., 2001), we performed Western blots for several of these antibodies and found that they are expressed in both salamander and mouse retinas (D.K., X.L., and E. Strehler, data not shown). From these results we can infer that antibodies used in these experiments are reacting with $Ca^{2+}$ transporters.

### SERCA2 is the dominant ER $Ca^{2+}$ sequestration mechanism in the salamander retina

The SERCA family consists of three isoforms (SERCA1–3), of which SERCA2 seems to predominate in most brain regions (Wu et al., 1995; Baba-Aissa et al., 1996). Alternative splicing of the SERCA2 gene produces two different splice variants (a and b), which differ in their turnover rates and their affinity for $Ca^{2+}$ (Verboomen et al., 1992; Wuytack et al., 2002). Sharply demarcated SERCA2a signals were detected at the level of inner segments (arrowheads in Fig. 2C). In addition, cell processes within the inner plexiform layer (IPL) were also immunopositive for SERCA2a. Moderate signal was seen in the outer plexiform layer (OPL), where dendritic processes from horizontal and bipolar cells receive input from photoreceptor terminals. Double-labeling of SERCA2a with SV2, a synaptic vesicle marker, showed substantial colocalization in the IPL (data not shown), suggesting that SERCA2a may

be expressed in synaptic processes of retinal neurons. Compared to the strong expression in the IPL, SERCA2a signal in the OPL was much weaker (Fig. 2C,D). In retinal sections we observed a modest degree of colocalization of SERCA2a with the presynaptic marker SV2 (not shown) and the cone photoreceptor marker calbindin (Fig. 2E; the synaptic terminals of cones in Fig. 2D,E are marked with arrowheads). An analysis of SERCA2a immunolabeling in isolated cone photoreceptors revealed that the signal is localized to the subellipsoid space and to the cell body (Fig. 2F), consistent with the known distribution of the ER cisternae in amphibian photoreceptors (Holtzman and Mercurio, 1980; Mercurio and Holtzman, 1982; Townes-Anderson et al., 1985).

SERCA2b is distributed across all classes of retinal neuron. As illustrated in Figure 3C, SERCA 2b is expressed in all retinal layers except in OSs. In addition to neurons, the SERCA2b antibody also labeled Müller cell processes in the proximal retina, as seen by colocalization with the Müller cell marker glutamine synthetase (GS; Fig. 3F—H). The intensity of SERCA2b signal in synaptic terminals of photoreceptors was weak, as seen in colocalization experiments with the synaptic vesicle marker SV2 (Fig. 3D,E). Instead, SERCA2b-immunopositive signals were confined to cell processes that surrounded photoreceptor terminals (arrowheads; Fig. 3E), possibly belonging to Müller cells and/or bipolar/horizontal cell processes. The most pronounced labeling was seen in the inner retina, indicating the highest concentration of SERCA2b in ganglion and amacrine cell processes. The antibody stained a GS-immunonegative compartment in the GCL, consistent with SERCA2b immunolocalization to GCL neurons (Fig. 3H). The SERCA2b antibody also stained cell bodies of presumed amacrine and bipolar cells. In addition, Müller cell processes and endfeet at the proximal edge of the GCL were labeled (arrowheads in Fig. 3F). The widespread localization of SERCA2b in the salamander retina is consistent with its ubiquitous localization in brain tissues (Baba-Aissa et al., 1996).

In contrast to the SERCA2 gene products, the SERCA3 transporters have a more limited distribution. SERCA3 is generally absent from neurons, with the exception of cerebellar Purkinje cells (Baba-Aissa et al., 1996). Immunostaining of the retina with the SERCA3 antibody showed moderate labeling across retinal layers. The cell bodies of photoreceptors, bipolar, and amacrine cells appeared to be labeled by the SERCA3 antibody (Fig. 3K). Especially prominent signal was seen in retinal Müller cells (arrowheads, Fig. 3K). To additionally test the specificity of the SERCA3 antibody, we co-applied it with PEP-015, a synthetic neutralizing peptide composed of the 11 amino acids from the amino terminal domain of the SERCA3 protein. Little SERCA3-immunopositive signal was detected in the presence of PEP-015. There was a faint signal in the OSs and ellipsoid regions of photoreceptors (Fig. 3L). This signal was similar to the staining observed in the absence of the primary antibody (Fig. 3J), suggesting that at these gain settings it originated from nonspecific staining of photoreceptor OSs and ellipsoids. Immunolabeling with a SERCA1 antibody produced no staining in the salamander retina (data not shown), consistent with previous results in studies of SERCA expression in the brain (Baba-Aissa et al., 1996). These results suggest that SERCA2 splice variants together with a minor contribution from SERCA3 account for most of $Ca^{2+}$ sequestration into retinal ER stores of tiger salamander.

## Ryanodine receptors are of the RyR2 isoform

Three RyR isoforms (RyR1–3), each a product of a different gene with the sequence homology of 66–70%, have been identified so far (Rossi and Sorrentino, 2002). An analysis of frog RyRs indicated the presence of two isoforms that correspond to the mammalian striated muscle and cardiac isoforms (RyR1 and RyR2; Lai et al., 1992). Thus, antibodies selective for RyR1 and RyR2 were used for immunostaining in salamander retina.

No immunostaining was seen with antibodies raised against RyR1 epitopes (data not shown). Three RyR2 antibodies, developed and characterized by F. Anthony Lai (Lai et al., 1992; Mackrill et al., 1997), were used, with identical results. Figure 4 shows a section of a salamander retina labeled with an antibody against the isoform 2 of the RyR family. The RyR2 immunostaining (Fig. 4B) resembled that obtained with the pan-RyR antibody (Križaj et al., 2003), suggesting that isoform 2 represents a major component of the RyR family expressed in the retina. Both pre- and postsynaptic domains of the OPL were stained with anti-RyR2, as seen by double-labeling with the synaptic marker SV2 (not shown), consistent with the idea that RyR2 are expressed in synaptic terminals as well as postsynaptically. A moderate RyR2 signal was observed in photoreceptor cell bodies, particularly in the subellipsoid space (arrows). Occasional amacrine and ganglion cell bodies were highly RyR2-immunopositive. The RyR2 antibody labeled AC and/or GC processes in the IPL as well as Müller cell endfeet and radial processes that span the INL (Fig. 4).

## $IP_3$ receptor localization in salamander

Cholinergic agonists, serotonin, norepinephrine, substance P, agonists of group I metabotropic glutamate receptors, as well as depolarization were all shown to stimulate $IP_3$ production in the retina (Gan and Iuvone, 1997; Osborne and Ghazi, 1990). Moreover, physiological experiments have suggested important roles for $IP_3$Rs in the function of retinal amacrine cells and ganglion cells (Akopian et al., 1998; Sosa et al., 2002). Three $IP_3$R isoforms have been identified so far with the type 1 receptor ($IP_3$R1) being the predominant neuronal isoform (Furuichi et al., 1993). However, in the salamander retina we detected no staining with antibodies raised against $IP_3$R1 epitopes (data not shown). In control experiments, the antibody raised against $IP_3$R1-labeled photoreceptor outer segments in the rat retina, consistent with the previous report by Wang et al. (1999; data not shown).

$IP_3$R2 is expressed in the salamander retina as well as in retinae of other vertebrates (rat, mouse, monkey; data not shown). As illustrated in Figure 5, antibody against $IP_3$R2-labeled cell bodies in the ONL, INL, and in the GCL. The subellipsoid space in photoreceptor inner segment was strongly immunoreactive for $IP_3$R2 (Fig. 5B), consistent with a high density of ER in this region (Mercurio and Holtzman, 1982;Townes-Anderson et al., 1985). $IP_3$R2 staining was also detected in the OPL (Fig. 5B,J– K). Little colocalization of $IP_3$R2 signal with the synaptic vesicle marker SV2 was observed (Fig. 5K), indicating that $IP_3$R2s were expressed in cells postsynaptic to photoreceptors. An extraordinarily intense $IP_3$R2 signal was often observed in salamander cones. Figure 5H illustrates a retinal section immunostained with anti-$IP_3$R2 antibody in which the signal from two photoreceptors is saturated. When the gain of the confocal system was decreased (Fig. 5I) the staining was revealed in a subpopulation of cone photoreceptors.

A subpopulation of amacrine cell bodies in the proximal INL was strongly $IP_3$R2-immunopositive (Fig. 5B,H). Likewise, the $IP_3$R2 antibody labeled several, but not all, cells in the GCL. Figure 5B shows a highly labeled cell next to a neighbor which did not exhibit an $IPR_3$ signal (arrowheads in Fig. 5A,B; see also Fig. 5H). We interpret these data as indicating that $IP_3$R2s regulate $Ca^{2+}$ signaling in a subset of amacrine cells and RGCs. $IP_3$R2 immunostaining was particularly prominent in the IPL, suggestive of $IP_3$ localization in processes of amacrine and/or ganglion cells. It remains to be determined whether the $IP_3$ receptors in the IPL are localized to terminals of bipolar cells (as suggested by Peng et al., 1991) and/or boutons of amacrine and ganglion cells (e.g., Lohmann et al., 2002). As a preliminary step toward identifying the subclasses of amacrine cells expressing $IP_3$R2, we double-immunostained the retinas with the antibody against tyrosine hydroxylase (TOH), a marker for dopaminergic amacrine cells (Witkovsky and Schütte, 1991). As seen in Figure 5E

—G, $IP_3R2$ colocalizes with TOH staining, suggesting that dopaminergic amacrine cells utilize $IP_3R2$-based $Ca^{2+}$ release from intracellular stores.

$IP_3R3$ is known to be expressed in pancreatic islets, kidney, and the gastrointestinal tract, but is found only in trace amounts in neurons (Sorrentino and Rizzuto, 2001). Consistent with a lack of $IP_3R3$ expression in neurons, no $IP_3R3$ signal was observed using this antibody (data not shown).

In conclusion, $IP_3R$ isoform 2, but not isoforms 1 or 3, is expressed in the retina of tiger salamander.

## PMCA1 is expressed in photoreceptors

The particular set of PMCA isoforms expressed in a given cell type may define the spatiotemporal pattern of $[Ca^{2+}]i$ response (e.g., Caride et al., 2001) and the ability of cells to respond to physiological stimuli (DeMarco et al., 2002). The PMCA family consists of four principal isoforms which differ in their affinities for $Ca^{2+}$ and calmodulin, ATP, and their susceptibility to phosphorylation by protein kinases A and C (Guerini, 1998; Strehler and Zacharias, 2001). When the salamander retina was immunostained with the 5F10 antibody that recognizes all isoforms of the PMCA family, all cell types within the retina were labeled (Fig. 6), suggesting that PMCAs are universally expressed in all classes of retinal neuron. The pan-PMCA antibody labeled cell bodies and ellipsoids of photoreceptors, the processes and cell bodies of Müller cells, as well as cell bodies and processes of bipolar, amacrine, and ganglion neurons. The most intense staining was observed in synaptic terminals of photoreceptors (arrowheads in Fig. 6) and in the IPL. These results are consistent with a ubiquitous expression of PMCAs in retinal cells.

To characterize the pattern of PMCA isoforms expressed in salamander retina we immunostained retinal sections with affinity-purified antibodies raised against rat and human epitopes (Filoteo et al., 1997; Swant Antibodies). Both classes of antibody yielded similar results. Figure 7B illustrates a confocal view of a section from salamander retina that was double-stained with the rabbit polyclonal antibody against PMCA1 (FITC signal) and the synaptic marker SV2 (Tx Red signal).

As seen in Figure 7B,D, the PMCA1 antibody immunostained the OPL of the retina (which consists of synaptic terminals of rod and cone photoreceptor and of dendrites of horizontal and bipolar cells). The PMCA1 signal enveloped the structures which were immunopositive for the synaptic marker SV2 (Fig. 7B), suggesting that they were selectively expressed in synaptic terminals of photoreceptors. At higher gain settings, PMCA1 staining was also detected in photoreceptor cell bodies. PMCA1 signal was much stronger in cone cell bodies than in rods. In tiger salamander, cone perikarya are found adjacent to the synaptic region, while rod perikarya are placed more distally (Lasansky, 1973). As seen in Figure 7D, a high intensity PMCA1 signal was detected in cones (arrows), whereas PMCA1 was more weakly expressed in the perikarya of rods (arrowheads; Fig. 7D). These results are consistent with physiological data obtained from $Ca^{2+}$ imaging studies on isolated salamander photoreceptors in which $Ca^{2+}$ extrusion from cone inner segments was shown to be much faster and more efficient compared to rod inner segments (Križaj and Copenhagen, 1998; Križaj et al., 2003).

Little PMCA1 signal was observed in the inner retina at confocal gain settings that were optimized for the signal expressed in the OPL (Fig. 7B). If, however, the confocal gain was increased, we could observe a signal within the IPL that exhibited a punctate pattern suggestive of localization to OFF bipolar cell terminals (Fig. 7D). Our results suggest, therefore, that $Ca^{2+}$ extrusion from tiger salamander photoreceptors and possibly from bipolar cells can be mediated by PMCA1.

### PMCA2 is highly expressed in the salamander retina

PMCA2, the PMCA isoform with the highest affinity for $Ca^{2+}$ (Guerini, 1998), is typically confined to neuronal tissues (Hammes et al., 1994; Stauffer et al., 1995; Zacharias et al., 1995). As illustrated in Figure 8, PMCA2 is also expressed in retinal neurons. The PMCA2 antibody labeled the cell bodies in the ONL and INL. A PMCA2-immunopositive signal was occasionally observed in outer segments of cones and in synaptic terminals of rods and cones, suggesting that PMCA2 can be expressed in a subset of photoreceptors. Plasma membranes of most, if not all, cells at the proximal edge of the INL were immunopositive for PMCA2, suggesting this high-affinity $Ca^{2+}$ transport system plays a key role in $Ca^{2+}$ extrusion from presumed amacrine cells. A prominent PMCA2 signal was also observed in cell processes in the IPL (Fig. 8B). Moreover, cell bodies in the GCL layer were often PMCA2-immunopositive (arrowheads in Fig. 8B).

### PMCA4 is localized to both synaptic layers, whereas PMCA3 is sparsely expressed in the IPL

Both PMCA3 and PMCA4 are also expressed in the retina of the tiger salamander. The PMCA3 isoform is strongly expressed in the IPL from the mouse retina (Križaj et al., 2002). In contrast, PMCA3 in the salamander retina is expressed in a sparse population of amacrine cells, the dendrites of which tended to ramify in the distal sublaminae of the IPL (Figs. 9B, 11G,H). Occasionally, a PMCA3-immunopositive ganglion cell was also observed. Figure 9E,F illustrates a GCL cell with a dendritic tree which ramified in the proximal IPL sublamina. Many of PMCA3-immunopositive GCL neurons exhibited regional variations of staining intensity; often, the primary dendrite was labeled more intensely compared to the rest of the cell (Fig. 9D).

Immunostaining with a monoclonal antibody raised against PMCA4 revealed that this $Ca^{2+}$ transporter is localized in both the inner and the outer synaptic layers (Fig. 10). PMCA4 was also expressed selectively in amacrine and ganglion cells. The localization of PMCA4 to inner retinal neurons is seen more clearly in Figure 11E—L for amacrine cells (Fig. 11E—H) and cells in GCL (Fig. I—L). To determine whether PMCA4 expression in photoreceptor terminals coincides with that of the PMCA1 (e.g., Fig. 7), we double-labeled the retina with PMCA1 and PMCA4 antibodies. PMCA4 strongly labeled synaptic terminals of photoreceptors and a substantial degree of colocalization with PMCA1 was observed (Fig. 11D). However, the distribution of PMCA4 did not colocalize point-to-point with that of PMCA1 (arrowheads in Fig. 11D), suggesting that both pump isoforms could contribute in an additive manner to $Ca^{2+}$ extrusion from photoreceptor terminals.

These results indicate that all PMCA isoforms are expressed in salamander inner retina. Based on the intensity of staining with the antibodies, we suggest that PMCA2 and PMCA4 are the predominant PMCA isoforms in the salamander retina, followed by PMCA1 and PMCA3.

### $Na^+/Ca^{2+}$ exchanger is localized to both plexiform layers

The second major plasma membrane $Ca^{2+}$ extrusion system is the $Na^+/Ca^{2+}$ exchanger (NCX). NCX often functions in parallel to PMCA-mediated $Ca^{2+}$ extrusion (Pozzan et al., 1994) and may be localized at the same or different sites in neuronal plasma membrane (Juhaszova et al., 2000). In contrast to PMCAs, the $Na^+/Ca^{2+}$ exchanger has a high capacity for $Ca^{2+}$ extrusion and is especially well suited for mass $Ca^{2+}$ extrusion following heavy $Ca^{2+}$ loads (Pozzan et al., 1994).

To determine distribution of NCXs in salamander retina we used a polyclonal antibody that has been shown to cross-react with amphibian and mammalian epitopes. Strong immunostaining of cell processes in the IPL and OPL was observed with this antibody (Fig. 12B). Double-labeling with calbindin, a marker for cone photoreceptors in the salamander

retina, confirmed postsynaptic localization of the NCX signal in the OPL (data not shown). Rarely (in one or two cells per section), cell bodies of amacrine cells with processes, which ramified within the distal IPL, were also labeled (Fig. 12C). To determine whether NCXs colocalize with PMCAs in dendritic compartments in the IPL, we double-immunostained the retina with the pan-PMCA antibody 5F10. Figure 12G depicts a high magnification view of salamander IPL double-stained with antibodies against NCX and pan-PMCA. Within the IPL, a significant amount of colocalized expression of PMCA and NCXs was observed. However, NCXs and PMCAs also exist in relatively distinct puncta isolated from each other (NCXs: arrowheads in Fig. 12E; PMCAs: arrows in Fig. 12F). Our results are consistent with a prominent role for Na+/$Ca^{2+}$ exchange in the inner retina (Gleason et al., 1995;Hurtado et al., 2002). They also suggest that PMCAs may act synergistically with NCXs to clear $Ca^{2+}$ loads during and following dendritic $Ca^{2+}$ signaling.

The NCX antibody also labeled a longitudinal structure within rod outer segments corresponding to the axonemal region (arrowheads in Fig. 12B; Fig. 12D; Whitehead et al., 1999). This signal was absent from control experiments in which the retina was labeled with secondary antibodies alone (not shown).

## DISCUSSION

We attempted to obtain a reasonably comprehensive overview of the cell-specific localization of $Ca^{2+}$ transporters in the salamander retina. The findings suggest that each class of retinal cell is endowed with a specific repertoire of $Ca^{2+}$ transporters. The diversity of $Ca^{2+}$ receptors and transporters observed provides a mechanistic basis for the remarkable divergence in $Ca^{2+}$ regulation and light response dynamics of retinal cells.

### Photoreceptors

Photoreceptors are formed by two structurally and functionally distinct compartments, the OS and the IS. $Ca^{2+}$ regulation in the OS is relatively well understood and molecular identities of major players in OS [$Ca^{2+}$]i homeostasis are known (reviewed in Fain et al., 2001). Compared to OSs, $Ca^{2+}$ transporters in photoreceptor ISs are not understood as well, even though $Ca^{2+}$ plays a prominent role in photoreceptor IS ion homeostasis (Križaj and Copenhagen, 2002). For example, $Ca^{2+}$ extrusion, in combination with $Ca^{2+}$ sequestration and influx is likely to set the steady-state [$Ca^{2+}$]i that controls many of key $Ca^{2+}$ dependent cellular enzymes (including $Ca^{2+}$-dependent protein kinases, phosphatases, lipases and the nitric oxide synthase; Križaj and Copenhagen, 2002). Moreover, small, light-evoked hyperpolarizations of rods and cones are associated with minute decreases in [$Ca^{2+}$]i (Rieke and Schwartz, 1996) and glutamate release (Witkovsky et al., 1997), possibly driven by high affinity $Ca^{2+}$ clearance mechanisms such as the PMCAs and SERCA pumps (Strehler and Zacharias, 2001). Here we report that PMCAs, SERCAs, $IP_3$Rs, and RyRs are prominently expressed within the photoreceptor IS.

PMCAs are the dominant $Ca^{2+}$ extrusion system in cells characterized by graded, sustained responses (i.e., photoreceptors, bipolar cells, and hair cells; Križaj and Copenhagen, 1998; Zenisek and Matthews, 2000; Yamoah et al., 1998). We showed recently that PMCAs play a crucial role in determining the time course of $Ca^{2+}$ clearance in rod and cone ISs (Križaj and Copenhagen, 1998; Križaj et al., 2003). Here we present evidence that PMCA1, PMCA2, and PMCA4 could all contribute to $Ca^{2+}$ extrusion from photoreceptor terminals and cell bodies. The immunostaining pattern in salamander photoreceptors was similar to that observed in the mammalian retina (Morgans et al., 1998; Križaj et al., 2002; Rentería et al., submitted). In the tree shrew, PMCAs are confined to the lateral walls of the synaptic terminal (Morgans et al., 1998), whereas in mouse (Križaj et al., 2002), rat (Renteria et al., submitted) and monkey (Križaj et al., 2002) PMCAs appear to be localized uniformly across the synaptic terminal.

This seems to mostly be the case in salamander as well (e.g., Figs. 6, 7). Regional variations in the intensity of PMCA staining in photoreceptor terminals and lateralized expression of PMCAs within photoreceptor terminals were occasionally observed. PMCA1 and PMCA4 were both expressed separately and/or colocalized within a given terminal and staining intensity for PMCA1, PMCA2, and PMCA4 varied between different terminals. The compartmentalization of PMCA1, PMCA2, and PMCA4 within synaptic subregions of rods and cones needs to be studied further in order to understand how $Ca^{2+}$ extrusion via different PMCAs can shape $Ca^{2+}$ homeostasis within a given rod and cone terminal.

Although both $IP_3$Rs and RyRs are known to play an important role in invertebrate photoreceptors (Walz et al., 1995; Arnon et al., 1997), their role in vertebrate photoreceptor function is not well understood (Križaj and Copenhagen, 2002). The photoreceptor cytoplasm is packed with ER cisternae (Mercurio and Holtzman, 1982) and our results are consistent with the idea that these structures contain abundant RyRs, $IP_3$Rs, and SERCA pumps. Previous physiological experiments suggested that RyR play a role in CICR and in modulation of synaptic transmission at the photoreceptor synapse, possibly via $Ca^{2+}$ release-mediated inactivation of presynaptic $Ca^{2+}$ channels (Križaj et al., 1999, 2003). As amphibian homologs of the mammalian RyR family are thought to possess very similar sensitivity to calcium, caffeine, and ryanodine (Lai et al., 1992; Fenelon and Pape, 2002), these studies predicted that the cardiac RyR isoform (homologous to the mammalian RyR2; Lai et al., 1992) would be found in photoreceptor ISs. Indeed, the staining results are consistent with RyR2 expression in these cells, suggesting this isoform could be responsible for CICR.

A key function for the $IP_3$R signaling cascade in vertebrate photoreceptors was suggested by the study of Jiang et al. (1996), who showed that retinae from PLC β4 knockout mice exhibit a 4-fold reduction in the amplitude of scotopic a and b wave components; paradoxically, recording from isolated rods showed little difference in light responses between null animals and littermate controls (Jiang et al., 1996). These findings suggested a post-phototransduction stage in which $IP_3$ release controls photoreceptor output. In addition, a role for $IP_3$ in the light adaptation of the photoreceptor OS phototransduction machinery has been proposed (Ghalayini and Anderson, 1984). However, the staining for $IP_3$Rs in photoreceptors has proved contradictory. Peng et al. (1991), using a pan-$IP_3$R antibody, found that $IP_3$ receptors are localized exclusively to synaptic terminals of salamander retinal neurons (including photoreceptors and bipolar cells). This finding was surprising, because most of the ER in photoreceptors is found in other subregions, particularly in the subellipsoid space, which is characterized by a dense accumulation of ER cisternae (Mercurio and Holtzman, 1982; Sjöstrand and Nilsson, 1965; Townes-Anderson et al., 1985). The $IP_3$R localization reported by Peng et al. (1991) suggested that the $Ca^{2+}$ stores within synaptic terminals of retinal neurons are specialized to participate in transmitter release (Peng et al., 1991). In contrast, a recent report (Wang et al., 1999) found the isoform 1 from the $IP_3$R family to be localized specifically to outer segments of rat and monkey cones. This finding also suggested that $IP_3$R1s are not expressed within the cone ER in a manner consistent with $IP_3$R1 distribution in the majority of other cell types (Pozzan et al., 1994; Berridge et al., 2003). Rather, Wang et al. (1999) suggested that $IP_3$Rs are localized to the plasma membrane of mammalian cones and thus play a nonconventional role in OS $Ca^{2+}$ homeostasis perhaps associated with the process of light adaptation (Wang et al., 1999). Here we report that salamander photoreceptors do express $IP_3$ receptors in a manner consistent with the widespread ramification of the cisternae of smooth ER in the subellipsoid space and the cell body (Mercurio and Holtzman, 1982; Sjöstrand and Nilsson, 1965). Relatively little $IP_3$R2 signal was observed in the synaptic terminal. $IP_3$R2s appeared to be particularly abundant in a subclass of cones. The specific $IP_3$R isoform or splice variant identified in salamander photoreceptors by Peng et al. (1991) therefore remains to be characterized. In preliminary experiments we confirmed the earlier report by Wang et al.

(1999) of the $IP_3R1$ immunostaining of rat cones but found no such signal in the salamander (data not shown).

SERCA transporters can play a crucial physiological role in photoreceptor $Ca^{2+}$ homeostasis, by collaborating with PMCAs to reduce the amplitude of depolarization-evoked $[Ca^{2+}]i$ transients within the cytoplasm (Križaj et al., 2003). Photoreceptors were found to express SERCA2 transporters of both "a" and "b" splice variants. SERCA2a signal detected at the level of ellipsoids was especially intriguing (Fig. 2). However, we were unable to unequivocally determine the compartment labeled by our SERCA2a antibody. Electron microscopy may be required to determine the precise localization of SERCA2a in the ONL.

## Bipolar cells

The synaptic connectivity and neurotransmitter profiles of salamander bipolar cells are different from those in mammalian retina (Wu et al., 2000; Yang et al., 2003). Nevertheless, our results suggest that salamander BCs, similarly to mammalian BCs (Križaj et al., 2002), express PMCA1 as well as PMCA2. Unlike the mouse retina (in which PMCA1 was strongly expressed in cell bodies and terminals of cone bipolar cells; Križaj et al., 2002), PMCA1 was not detected in salamander INL. Moreover, the PMCA1 signal in the salamander IPL was moderate compared to that observed in the mammalian retinae. Most, if not all, bipolar cell bodies in salamander expressed PMCA2; moreover, many salamander BCs also seemed to express moderate amounts of PMCA4. SERCA immunostaining suggests that salamander bipolar cells express SERCA2b and possibly SERCA3 isoforms.

## Amacrine cells and ganglion cells

Recent reports suggested that intracellular calcium plays a key role in amacrine cell function (Akopian and Witkovsky, 2002; Hurtado et al., 2002); however, the isoform identity of $Ca^{2+}$ transporters that underlie $Ca^{2+}$ signaling has not been addressed. We report here that amacrine cells in this amphibian express a wide variety of $Ca^{2+}$ transporters and that some $Ca^{2+}$ transporters are localized to cell bodies of specific amacrine and ganglion neurons. Plasma membrane transporters PMCA2-4, NCX1, and possibly PMCA1 are expressed in salamander ACs. In addition, $Ca^{2+}$ store transporters SERCA2a, 2b, and 3, $IP_3R2$ and RyR2 are also found in these cells. Although we did not perform colocalization studies for the immunoreactivity of various isoform combinations, the sparsity of staining and differences in cell morphologies leads us to the idea that different classes of amacrine and ganglion cells might express different sets of $Ca^{2+}$ transporters. Whereas PMCA3, PMCA4, RyRs, NCXs, and $IP_3Rs$ were strongly expressed within small subsets of AC and GC bodies, SERCA2b and PMCA2 were expressed in the majority of these cells. These data are consistent with large morphological and functional differences between populations of amacrine cells (Masland, 1996; Gabriel et al., 2000). For example, in rat, different ganglion cells were shown to possess different types of metabotropic glutamate receptors including those (e.g., mGluR1 and mGluR5) whose activation is coupled to turnover of phosphoinositides and generation of $IP_3$ (Hartveit et al., 1995; Koulen et al., 1997).

We detected intense $IP_3R2$ labeling in the plasma membrane of a subset of amacrine and ganglion cell bodies (which include those of tyrosine hydroxylase immunopositive neurons), suggesting that $IP_3$ isoform 2 receptors are localized to subsurface cisternae in amacrine and ganglion neurons. Subsurface cisternae are ER structures localized within nm of the plasma membrane and thus well positioned to modulate $Ca^{2+}$-dependent signaling at the plasma membrane. The diffuse labeling of the IPL with the $IP_3R2$ antibody is consistent with the distribution of group I metabotropic receptors in rat (Koulen et al., 1997) and chick retina (Sosa et al., 2002) as well as with the expression of cholinergic and peptidergic receptors in retinal amacrine cells (Osborne and Ghazi, 1990). These receptors are often linked to activation

of phospholipase C and subsequent generation of $IP_3$. In turn, $Ca^{2+}$ released from $IP_3$-sensitive stores was shown to have a variety of physiological effects in inner retinal neurons, including a reduction in affinity of metabotropic $GABA_B$ receptors in salamander ganglion cells (Shen and Slaughter, 1999), suppression of current flow through $GABA_A$ receptors in turtle ganglion cells (Akopian et al., 1998) and a decrease in NMDA receptor-gated channel activity in salamander ganglion cells (Akopian and Witkovsky, 2001). These physiological studies suggested that IP-mediated $Ca^{2+}$ release occurs in many, if not all, retinal ganglion cells. Our data is consistent with the interpretation that $IP_3R2$ represent the predominant $IP_3R$ isoform in the salamander retina. The results indicate that levels of $IP_3R2$ expression are significantly higher in a subset of ganglion cells; however, weak $IP_3R2$ signal was detected at high gain in the majority of ganglion cells (data not shown). Our results predict that PLC-coupled $Ca^{2+}$ release will be more pronounced in a subset of retinal ganglion cells. Consistent with results from Wang et al. (1999), little specific signal was detected in the inner retina using $IP_3R1$ and $IP_3R3$ antibodies. Since electrophysiological studies indicate that most, if not all, spiking neurons express $IP_3Rs$ (Akopian and Witkovsky, 2001) it is possible that, using our antibodies, we missed $IP_3R1s$ and $IP_3R3s$ that may be expressed in these cells. Alternatively, relatively low levels of $IP_3R2$ could be responsible for mediating cell responses observed in physiological studies (Shen and Slaughter, 1999; Akopian and Witkovsky, 2001).

Our data is also consistent with the large differences in plasma membrane $Ca^{2+}$ extrusion systems observed in amacrine cells. Unlike photoreceptors and bipolar cells in which PMCA-mediated $Ca^{2+}$ extrusion predominates (Križaj and Copenhagen, 1998; Zenisek and Matthews, 2000), $Ca^{2+}$ clearance from cytoplasm of amacrine and ganglion cells is supported by both NCXs and PMCAs; the PMCA contribution encompasses the range from 0% to ~75% (Gleason et al., 1995; Bindokas et al., 1994). Activation of PMCAs and NCXs defines the spatial and temporal patterns of $Ca^{2+}$ release from internal stores (Hurtado et al., 2002) as well as the dynamics of amacrine synaptic transmission (Gleason et al., 1995). Our results suggest that NCXs are strongly expressed in amacrine/ganglion cell processes, although, very occasionally, an amacrine cell body was also intensely stained with the NCX antibody. In the IPL, NCXs colocalized with PMCAs at some, but not all, puncta. The relative intensities of NCX- and PMCA-specific signals varied widely among cells, suggesting different arrays of available $Ca^{2+}$ extrusion mechanisms in dendritic processes of inner retinal neurons. A similar conclusion about differential expression of PMCAs and NCXs has been reached in physiological experiments (Gleason et al., 1995; Hurtado et al., 2002). Our results suggest that many of such interactions are likely to involve PMCA2, which is expressed in most AC and GC bodies and processes, and appears to be a major $Ca^{2+}$ extrusion system in the inner retina of the tiger salamander and the mouse (Duncan et al., 2004). Since PMCA2 possess the highest affinity for $Ca^{2+}$ of all $Ca^{2+}$ pumps (Guerini, 1998; Strehler and Zacharias, 2001), this suggests a need for precise tuning of $[Ca^{2+}]i$ in the amacrine and ganglion cells. Interestingly, PMCA3, which is found in the majority of amacrine and ganglion neurons in mouse (Križaj et al., 2002), rat (Copenhagen et al., 2003), and monkey retinae (D. Križaj, unpublished observation), appears to be restricted to sparse subpopulations of salamander amacrine and/or ganglion cells. PMCA1 and PMCA3 expression in the inner retina of salamander is significantly weaker compared to mammals.

We did not examine the distribution of NCX isoforms in this project. Our NCX antibody recognizes best the NCX1 isoform of the NCX receptor (Philipson et al., 1988); however, it is also thought to cross-react with the other two NCX isoforms (Yip et al., 1992). More specific identification of NCX isoform localization in the retina awaits further studies using isoform-specific antibodies.

### SERCAs

We found that the SERCA2 isoform, which is phylogenetically the oldest, is by far the most widespread of all SERCA isoforms in the retina. This result is consistent with the ubiquitous expression of SERCA2 in the brain (Wuytack et al., 1989; Baba-Aissa et al., 1996). Of the two SERCA2 splice variants, the "b" variant is expressed in many retinal cells, consistent with its accepted role as the "housekeeping $Ca^{2+}$ ATPase" (Wuytack et al., 2002). SERCA2b staining was especially intense in Müller cell endfeet and proximal processes, indicating a role for $Ca^{2+}$ stores in regulation of $Ca^{2+}$ waves and neuronal-glial interactions (Newman, 2001). Expression of SERCA2a in the retina is unconventional, because (with the exception of cerebellar Purkinje cells) SERCA2a is typically not found in neurons (Baba-Aissa et al., 1996). The localization of SERCA2a was much more restricted compared to that of SERCA2b. In particular, a strongly demarcated SERCA2a signal was observed at the level of photoreceptor ellipsoids. Densely packed cisternae of ER are found in this region together with a high density of mitochondria (Holtzman and Mercurio, 1982; Townes-Anderson, 1995). SERCA2a may thus play a role in ER-mitochondrial interactions in the inner segment (Križaj et al., 2003).

### Functional implications of $Ca^{2+}$ transporter localization in the retina

The low coefficient of diffusion of $Ca^{2+}$ in the cytoplasm ($\sim 10^{-7}$ $cm^2s^{-1}$ compared to $\sim 10^{-5}$ $cm^2s^{-1}$ for $Na^+$; Kushmerick and Podolsky, 1969; Nakatani et al., 2002) and the high density of immobile $Ca^{2+}$-binding proteins in many retinal cells (Deng et al., 2001), including photoreceptors (Lagnado et al., 1992; Nakatani et al., 2002) suggest that calcium regulation in retinal cells may often depend on local distribution of $Ca^{2+}$ buffers and transporters rather than on active propagation of $Ca^{2+}$ signals from the cell body into dendritic spines and vice versa (Hurtado et al., 2002; Euler et al., 2002; Ciccolini et al., 2003). The immunostaining for SERCAs, $IP_3$Rs, and RyRs in the salamander retina is consistent with the dominant role for ER in regulation of retinal cell $[Ca^{2+}]i$ (Hurtado et al., 2002; Križaj et al., 2003). $Ca^{2+}$-sequestering compartments and buffers can increase the apparent $Ca^{2+}$ diffusion coefficient by at least an order of magnitude (Albritton et al., 1992; Al-Baldawi and Abercrombie, 1995) and thus significantly influence $Ca^{2+}$ signaling within different cytoplasmic compartments. A given set of $Ca^{2+}$ transporters localized to the plasma membrane, ER, and mitochondria is thus likely to endow retinal cells with specific repertoires of intrinsic activity, $[Ca^{2+}]i$ responses to light and/or neuromodulatory stimulation. The ability of $Ca^{2+}$ transporters to be at once ubiquitously expressed but nevertheless provide highly specific spatiotemporal $[Ca^{2+}]i$ signals has been attributed to the diversity of expression of different transporter isoforms (Sharp et al., 1999), subcellular distributions of $Ca^{2+}$ transporters (Berridge et al., 2003; Laflamme et al., 2002; Chicka and Strehler, 2003) and complex regulation of the transporters by calmodulin, protein kinases, and other modulatory factors (Strehler and Zacharias, 2001). Consistent with that notion we found that different classes of retinal neurons possess different $Ca^{2+}$-signaling "toolkits" (Berridge et al., 2003), i.e., widely differing combinations of $Ca^{2+}$ transporters (NCXs, SERCAs, PMCAs, RyRs, and $IP_3$Rs). Indeed, hot-spots of $[Ca^{2+}]i$ observed in amacrine cell dendrites during stimulation (Euler et al., 2002; Hurtado et al., 2002) are consistent with the idea that these cells possess signaling microdomains formed by strategic placement of $Ca^{2+}$ influx, extrusion, and sequestration mechanisms The results presented here suggest a structural basis for such signaling microdomains consisting of $Ca^{2+}$ pumps, exchangers, and $Ca^{2+}$ release channels in the retina. The localization data also provide immunohistochemical foundation for physiological experiments which showed that release of $Ca^{2+}$ from intracellular stores regulates a wide variety of retinal pathways, including those that regulate transmitter release (Križaj et al., 1999), GABAergic neurotransmission (Akopian and Witkovsky, 1998; Shen and Slaughter, 1999; Ciccolini et al., 2003), dendritic growth (Lohmann et al., 2002) and $Ca^{2+}$ oscillations (Newman, 2001). They also support the hypothesis that ER could represent a main site for dynamic control of cellular $[Ca^{2+}]i$ by acting as an integrator and amplifier of $Ca^{2+}$ influx (Nakamura et al., 1999; Majewska et al., 2000;

Hurtado et al., 2002; Berridge et al., 2003) and that $Ca^{2+}$ release from $Ca^{2+}$ stores could play a role in shaping of the visual signal (Križaj et al., 1999; Akopian and Witkovsky, 2001; Hurtado et al., 2002).

In conclusion, the findings in this article suggest a refinement of the simple schema according to which $Ca^{2+}$ regulation in retinal neurons consists of $Ca^{2+}$ influx through voltage-gated $Ca^{2+}$ channels and extrusion across the plasma membrane. Instead, a wide variety of $Ca^{2+}$ transporters and their associated proteins is specifically assembled in order to fulfill a need for fine-tuning of spatially restricted $[Ca^{2+}]i$ changes in retinal cells.

## ACKNOWLEDGMENTS

We thank Dr. Emanuel Strehler and Dr. Rene Rentería for helpful discussions and Dr. Frank Wuytack (Katholieke Universiteit Leiden), Dr. John Penniston (Mayo Clinic), and Dr. F. Anthony Lai (University College of Wales) for generous gifts of antibodies. We thank Ms. Anne Schreiber and Mr. Edwin Dumlao for expert technical assistance.

Grant sponsor: National Institutes of Health; Grant number: EY 13870 (D.K.), EY 01869 (D.R.C.); Grant sponsor: That Man May See; Grant sponsor: University of California, San Francisco Academic Senate award (D.K.).

## LITERATURE CITED

Akopian A, Witkovsky P. Intracellular calcium reduces light-induced excitatory post-synaptic responses in salamander retinal ganglion cells. J Physiol 2001;532:43–53. [PubMed: 11283224]

Akopian A, Witkovsky P. Calcium and retinal function. Mol Neurobiol 2002;25:113–132. [PubMed: 11936555]

Akopian A, Gabriel R, Witkovsky P. Calcium released from intracellular stores inhibits GABAA-mediated currents in ganglion cells of the turtle retina. J Neurophysiol 1998;80:1105–1115. [PubMed: 9744925]

al-Baldawi NF, Abercrombie RF. Calcium diffusion coefficient in Myxicola axoplasm. Cell Calcium 1995;17:422–430. [PubMed: 8521456]

Albritton NL, Meyer T, Stryer L. Range of messenger action of calcium ion and inositol 1,4,5-trisphosphate. Science 1992;258:1812–1815. [PubMed: 1465619]

Arnon A, Cook B, Gillo B, Montell C, Selinger Z, Minke B. Calmodulin regulation of light adaptation and store-operated dark current in Drosophila photoreceptors. Proc Natl Acad Sci USA 1997;94:5894–5899. [PubMed: 9159171]

Baba-Aissa F, Raeymaekers L, Wuytack F, De Greef C, Missiaen L, Casteels R. Distribution of the organellar $Ca^{2+}$ transport ATPase SERCA2 isoforms in the cat brain. Brain Res 1996;743:141–153. [PubMed: 9017241]

Berridge MJ, Bootman MD, Roderick HL. Calcium signalling: dynamics, homeostasis and remodelling. Nat Rev Mol Cell Biol 2003;4:517–529. [PubMed: 12838335]

Bindokas VP, Yoshikawa M, Ishida AT. $Na^{(+)}$-$Ca^{2+}$ exchanger-like immunoreactivity and regulation of intracellular $Ca^{2+}$ levels in fish retinal ganglion cells. J Neurophysiol 1994;72:47–55. [PubMed: 7965029]

Capovilla M, Hare WA, Owen WG. Voltage gain of signal transfer from retinal rods to bipolar cells in the tiger salamander. J Physiol 1987;391:125–140. [PubMed: 3443944]

Caride AJ, Filoteo AG, Penheiter AR, Paszty K, Enyedi A, Penniston JT. Delayed activation of the plasma membrane calcium pump by a sudden increase in $Ca^{2+}$: fast pumps reside in fast cells. Cell Calcium 2001;30:49–57. [PubMed: 11396987]

Chicka MC, Strehler EE. Alternative splicing of the first intracellular loop of plasma membrane $Ca^{2+}$-ATPase isoform 2 alters its membrane targeting. J Biol Chem 2003;278:18464–18470. [PubMed: 12624087]

Ciccolini F, Collins TJ, Sudhoelter J, Lipp P, Berridge MJ, Bootman MD. Local and global spontaneous calcium events regulate neurite outgrowth and onset of GABAergic phenotype during neural precursor differentiation. J Neurosci 2003;23:103–111. [PubMed: 12514206]

Delmas P, Brown DA. Junctional signaling microdomains: bridging the gap between the neuronal cell surface and $Ca^{2+}$ stores. Neuron 2002;36:787–790. [PubMed: 12467583]

DeMarco SJ, Chicka MC, Strehler EE. Plasma membrane $Ca^{2+}$ ATPase isoform 2b interacts preferentially with $Na^{+}/H^{+}$ exchanger regulatory factor 2 in apical plasma membranes. J Biol Chem 2002;277:10506–10511. [PubMed: 11786550]

Deng P, Cuenca N, Doerr T, Pow DV, Miller R, Kolb H. Localization of neurotransmitters and calcium binding proteins to neurons of salamander and mudpuppy retinas. Vision Res 2001;41:1771–1783. [PubMed: 11369041]

Euler T, Detwiler PB, Denk W. Directionally selective calcium signals in dendrites of starburst amacrine cells. Nature 2002;418:845–852. [PubMed: 12192402]

Fain GL, Matthews HR, Cornwall MC, Koutalos Y. Adaptation in vertebrate photoreceptors. Physiol Rev 2001;81:117–151. [PubMed: 11152756]

Fenelon K, Pape PC. Recruitment of $Ca^{(2+)}$ release channels by calcium-induced $Ca^{(2+)}$ release does not appear to occur in isolated $Ca^{(2+)}$ release sites in frog skeletal muscle. J Physiol 2002;544:777–791. [PubMed: 12411523]

Filoteo AG, Elwess NL, Enyedi A, Caride A, Aung HH, Penniston JT. Plasma membrane $Ca^{2+}$ pump in rat brain. Patterns of alternative splices seen by isoform-specific antibodies. J Biol Chem 1997;272:23741–23747. [PubMed: 9295318]

Furuichi T, Simon-Chazottes D, Fujino I, Yamada N, Hasegawa M, Miyawaki A, Yoshikawa S, Guenet JL, Mikoshiba K. Widespread expression of inositol 1,4,5-trisphosphate receptor type 1 gene (Insp3r1) in the mouse central nervous system. Receptors Channels 1993;1:11–24. [PubMed: 8081710]

Gabriel R, Rabl K, Veisenberger E. Synaptology of the inner plexiform layer in the anuran retina. Microsc Res Tech 2000;50:394–402. [PubMed: 10941175]

Gan J, Iuvone PM. Depolarization and activation of dihydropyridine-sensitive $Ca^{2+}$ channels stimulate inositol phosphate accumulation in photoreceptor-enriched chick retinal cell cultures. J Neurochem 1997;68:2300–2307. [PubMed: 9166722]

Ghalayini A, Anderson RE. Phosphatidylinositol 4,5-bisphosphate: light-mediated breakdown in the vertebrate retina. Biochem Biophys Res Commun 1984;124:503–506. [PubMed: 6093803]

Gleason E, Borges S, Wilson M. Electrogenic Na-Ca exchange clears $Ca^{2+}$ loads from retinal amacrine cells in culture. J Neurosci 1995;15:3612–3621. [PubMed: 7751933]

Guerini D. The significance of the isoforms of plasma membrane calcium ATPase. Cell Tissue Res 1998;292:191–197. [PubMed: 9560462]

Hammes A, Oberdorf S, Strehler EE, Stauffer T, Carafoli E, Vetter H, Neyses L. Differentiation-specific isoform mRNA expression of the calmodulin-dependent plasma membrane $Ca^{(2+)}$-ATPase. FASEB J 1994;8:428–435. [PubMed: 8168693]

Hartveit E, Brandstatter JH, Enz R, Wassle H. Expression of the mRNA of seven metabotropic glutamate receptors (mGluR1 to 7) in the rat retina. An in situ hybridization study on tissue sections and isolated cells. Eur J Neurosci 1995;7:1472–1483. [PubMed: 7551173]

Holtzman E, Mercurio AM. Membrane circulation in neurons and photoreceptors: some unresolved issues. Int Rev Cytol 1980;67:1–67. [PubMed: 6161097]

Hurtado J, Borges S, Wilson M. $Na^{(+)}$-$Ca^{(2+)}$ exchanger controls the gain of the $Ca^{(2+)}$ amplifier in the dendrites of amacrine cells. J Neurophysiol 2002;88:2765–2777. [PubMed: 12424311]

Jiang H, Lyubarsky A, Dodd R, Vardi N, Pugh E, Baylor D, Simon MI, Wu D. Phospholipase C beta 4 is involved in modulating the visual response in mice. Proc Natl Acad Sci USA 1996;93:14598–14601. [PubMed: 8962098]

Juhaszova M, Church P, Blaustein MP, Stanley EF. Location of calcium transporters at presynaptic terminals. Eur J Neurosci 2000;12:839–846. [PubMed: 10762313]

Keirstead SA, Miller RF. Calcium waves in dissociated retinal glial (Müller) cells are evoked by release of calcium from intracellular stores. Glia 1995;14:14–22. [PubMed: 7615342]

Križaj D, Copenhagen DR. Compartmentalization of calcium extrusion mechanisms in the outer and inner segments of photoreceptors. Neuron 1998;21:249–256. [PubMed: 9697868]

Križaj D, Copenhagen DR. Calcium regulation in photoreceptors. Front Biosci 2002;7:d2023–2044. [PubMed: 12161344]

Križaj D, Bao JX, Schmitz Y, Witkovsky P, Copenhagen DR. Caffeine-sensitive calcium stores regulate synaptic transmission from retinal rod photoreceptors. J Neurosci 1999;19:7249–7261. [PubMed: 10460231]

Križaj D, Demarco SJ, Johnson J, Strehler EE, Copenhagen DR. Cell-specific expression of plasma membrane calcium ATPase isoforms in retinal neurons. J Comp Neurol 2002;451:1–21. [PubMed: 12209837]

Križaj D, Lai FA, Copenhagen DR. Ryanodine stores and calcium regulation in the inner segments of salamander rods and cones. J Physiol 2003;547:761–774. [PubMed: 12562925]

Kushmerick MJ, Podolsky RJ. Ionic mobility in muscle cells. Science 1969;166:1297–1298. [PubMed: 5350329]

Laflamme K, Domingue O, Guillemette BI, Guillemette G. Immunohistochemical localization of type 2 inositol 1,4,5-trisphosphate receptor to the nucleus of different mammalian cells. J Cell Biochem 2002;85:219–228. [PubMed: 11891865]

Lagnado L, Cervetto L, McNaughton PA. Calcium homeostasis in the outer segments of retinal rods from the tiger salamander. J Physiol 1992;455:111–142. [PubMed: 1282928]

Lai FA, Liu QY, Xu L, el-Hashem A, Kramarcy NR, Sealock R, Meissner G. Amphibian ryanodine receptor isoforms are related to those of mammalian skeletal or cardiac muscle. Am J Physiol 1992;263:C365–372. [PubMed: 1325114]

Lamb TD, Pugh EN Jr. A quantitative account of the activation steps involved in phototransduction in amphibian photoreceptors. J Physiol 1992;449:719–758. [PubMed: 1326052]

Lasansky A. Organization of the outer synaptic layer in the retina of the larval tiger salamander. Philos Trans R Soc Lond B Biol Sci 1973;265:471–489. [PubMed: 4147132]

Lohmann C, Myhr KL, Wong RO. Transmitter-evoked local calcium release stabilizes developing dendrites. Nature 2002;418:177–181. [PubMed: 12110889]

Lukasiewicz PD, Maple BR, Werblin FS. A novel GABA receptor on bipolar cell terminals in the tiger salamander retina. J Neurosci 1994;14:1202–1212. [PubMed: 8120620]

Mackrill JJ, Challiss RA, O'Connell DA, Lai FA, Nahorski SR. Differential expression and regulation of ryanodine receptor and myoinositol 1,4,5-trisphosphate receptor $Ca^{2+}$ release channels in mammalian tissues and cell lines. Biochem J 1997;327(Pt 1):251–258. [PubMed: 9355760]

Majewska A, Brown E, Ross J, Yuste R. Mechanisms of calcium decay kinetics in hippocampal spines: role of spine calcium pumps and calcium diffusion through the spine neck in biochemical compartmentalization. J Neurosci 2000;20:1722–1734. [PubMed: 10684874]

Martin V, Bredoux R, Corvazier E, Van Gorp R, Kovacs T, Gelebart P, Enouf J. Three novel sarco/endoplasmic reticulum Ca2+-ATPase (SERCA) 3 isoforms. Expression, regulation, and function of the membranes of the SERCA3 family. J Biol Chem 2002;277:24442–24452. [PubMed: 11956212]

Masland RH. Processing and encoding of visual information in the retina. Curr Opin Neurobiol 1996;6:467–474. [PubMed: 8794095]

Meister M, Lagnado L, Baylor DA. Concerted signaling by retinal ganglion cells. Science 1995;270:1207–1210. [PubMed: 7502047]

Mercurio AM, Holtzman E. Smooth endoplasmic reticulum and other agranular reticulum in frog retinal photoreceptors. J Neurocytol 1982;11:263–293. [PubMed: 6978386]

Micci MA, Christensen BN. $Na^{+}/Ca^{2+}$ exchange in catfish retina horizontal cells: regulation of intracellular $Ca^{2+}$ store function. Am J Physiol 1998;274:C1625–1633. [PubMed: 9611128]

Nakamura T, Barbara JG, Nakamura K, Ross WN. Synergistic release of $Ca^{2+}$ from IP3-sensitive stores evoked by synaptic activation of mGluRs paired with backpropagating action potentials. Neuron 1999;24:727–737. [PubMed: 10595522]

Morgans CW, El Far O, Berntson A, Wässle H, Taylor WR. Calcium extrusion from mammalian photoreceptor terminals. J Neurosci 1998;18:2467–2474. [PubMed: 9502807]

Nakatani K, Chen C, Koutalos Y. Calcium diffusion coefficient in rod photoreceptor outer segments. Biophys J 2002;82:728–739. [PubMed: 11806915]

Newman EA. Calcium signaling in retinal glial cells and its effect on neuronal activity. Prog Brain Res 2001;132:241–254. [PubMed: 11544993]

Osborne NN, Ghazi H. Agonist-stimulated inositol phospholipid hydrolysis in the mammalian retina. Prog Retinal Res 1990;10:101–134.

Peng YW, Sharp AH, Snyder SH, Yau KW. Localization of the inositol 1,4,5-trisphosphate receptor in synaptic terminals in the vertebrate retina. Neuron 1991;6:525–531. [PubMed: 1849721]

Philipson KD, Longoni S, Ward R. Purification of the cardiac $Na^{+}$Ca2+ exchange protein. Biochim Biophys Acta 1988;945:298–306. [PubMed: 3191125]

Pozzan T, Rizzuto R, Volpe P, Meldolesi J. Molecular and cellular physiology of intracellular calcium stores. Physiol Rev 1994;74:595–636. [PubMed: 8036248]

Rieke F, Schwartz EA. Asynchronous transmitter release: control of exocytosis and endocytosis at the salamander rod synapse. J Physiol 1996;493(Pt 1):1–8. [PubMed: 8735690]

Rossi D, Sorrentino V. Molecular genetics of ryanodine receptors $Ca^{(2+)}$-release channels. Cell Calcium 2002;32:307–319. [PubMed: 12543091]

Sherry DM, Yang H, Standifer KM. Vesicle-associated membrane protein isoforms in the tiger salamander retina. J Comp Neurol 2001;431:424–436. [PubMed: 11223812]

Solessio E, Lasater EM. Calcium-induced calcium release and calcium buffering in retinal horizontal cells. Vis Neurosci 2002;19:713–725. [PubMed: 12688667]

Sosa R, Hoffpauir B, Rankin ML, Bruch RC, Gleason EL. Metabotropic glutamate receptor 5 and calcium signaling in retinal amacrine cells. J Neurochem 2002;81:973–983. [PubMed: 12065609]

Stauffer TP, Guerini D, Carafoli E. Tissue distribution of the four gene products of the plasma membrane $Ca^{2+}$ pump. A study using specific antibodies. J Biol Chem 1995;270:12184–12190. [PubMed: 7538133]

Strehler EE, Zacharias DA. Role of alternative splicing in generating isoform diversity among plasma membrane calcium pumps. Physiol Rev 2001;81:21–50. [PubMed: 11152753]

Sugioka M, Fukuda Y, Yamashita M. Development of glutamateinduced intracellular $Ca^{2+}$ rise in the embryonic chick retina. J Neurobiol 1998;34:113–125. [PubMed: 9468383]

Townes-Anderson E, MacLeish PR, Raviola E. Rod cells dissociated from mature salamander retina: ultrastructure and uptake of horse-radish peroxidase. J Cell Biol 1985;100:175–188. [PubMed: 3965470]

Walz B, Baumann O, Zimmermann B, Ciriacy-Wantrup EV. Caffeine- and ryanodine-sensitive $Ca^{(2+)}$-induced $Ca^{2+}$ release from the endoplasmic reticulum in honeybee photoreceptors. J Gen Physiol 1995;105:537–567. [PubMed: 7608657]

Wang TL, Sterling P, Vardi N. Localization of type I inositol 1,4,5-triphosphate receptor in the outer segments of mammalian cones. J Neurosci 1999;19:4221–4228. [PubMed: 10341226]

Wei SK, Ruknudin A, Hanlon SU, McCurley JM, Schulze DH, Haigney MC. Protein kinase A hyperphosphorylation increases basal current but decreases beta-adrenergic responsiveness of the sarcolemmal Na+-Ca2+ exchanger in failing pig myocytes. Circ Res 2003;92:897–903. [PubMed: 12676818]

Wellis DP, Werblin FS. Dopamine modulates GABAc receptors mediating inhibition of calcium entry into and transmitter release from bipolar cell terminals in tiger salamander retina. J Neurosci 1995;15:4748–761. [PubMed: 7623108]

Werblin FS, Dowling JE. Organization of the retina of the mudpuppy, Necturus maculosus. II. Intracellular recording. J Neurophysiol 1969;32:339–355. [PubMed: 4306897]

Witkovsky P, Schmitz Y, Akopian A, Križaj D, Tranchina D. Gain of rod to horizontal cell synaptic transfer: relation to glutamate release and a dihydropyridine-sensitive calcium current. J Neurosci 1997;17:7297–7306. [PubMed: 9295376]

Wu SM. Input-output relations of the feedback synapse between horizontal cells and cones in the tiger salamander retina. J Neurophysiol 1991;65:1197–1206. [PubMed: 1651374]

Wu SM, Gao F, Maple BR. Functional architecture of synapses in the inner retina: segregation of visual signals by stratification of bipolar cell axon terminals. J Neurosci 2000;20:4462–4470. [PubMed: 10844015]

Wuytack F, Eggermont JA, Raeymaekers L, Plessers L, Casteels R. Antibodies against the non-muscle isoform of the endoplasmic reticulum Ca2(+)-transport ATPase. Biochem J 1989;264:765–769. [PubMed: 2482734]

Wuytack F, Papp B, Verboomen H, Raeymaekers L, Dode L, Bobe R, Enouf J, Bokkala S, Authi KS, Casteels R. A sarco/endoplasmic reticulum $Ca^{(2+)}$-ATPase 3-type $Ca^{2+}$ pump is expressed in platelets, in lymphoid cells, and in mast cells. J Biol Chem 1994;269:1410–1416. [PubMed: 8288608]

Wuytack F, Raeymaekers L, Missiaen L. Molecular physiology of the SERCA and SPCA pumps. Cell Calcium 2002;32:279–305. [PubMed: 12543090]

Yamoah EN, Lumpkin EA, Dumont RA, Smith PJ, Hudspeth AJ, Gillespie PG. Plasma membrane $Ca^{2+}$-ATPase extrudes $Ca^{2+}$ from hair cell stereocilia. J Neurosci 1998;18:610–624. [PubMed: 9425003]

Yang CY, Zhang J, Yazulla S. Differential synaptic organization of GABAergic bipolar cells and non-GABAergic (glutamatergic) bipolar cells in the tiger salamander retina. J Comp Neurol 2003;455:187–197. [PubMed: 12454984]

Yip RK, Blaustein MP, Philipson KD. Immunologic identification of Na/Ca exchange protein in rat brain synaptic plasma membrane. Neurosci Lett 1992;136:123–126. [PubMed: 1378951]

Zacharias DA, Dalrymple SJ, Strehler EE. Transcript distribution of plasma membrane $Ca^{2+}$ pump isoforms and splice variants in the human brain. Brain Res Mol Brain Res 1995;28:263–272. [PubMed: 7723625]

Zenisek D, Matthews G. The role of mitochondria in presynaptic calcium handling at a ribbon synapse. Neuron 2000;25:229–237. [PubMed: 10707986]

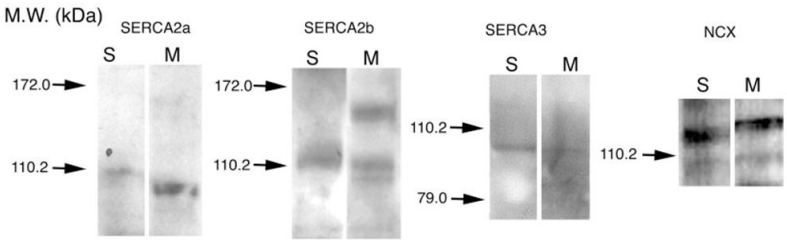


**Fig. 1.**

Representative Western blots of SERCA2a, SERCA2b, SERCA3, and NCX proteins in salamander and mouse retinae. Total protein lysates (15–25 mg protein per lane) were processed for Western blotting by using specific antibodies. Molecular weight (MW) standards are indicated in kilodaltons (kDa) on the side and marked by arrows.

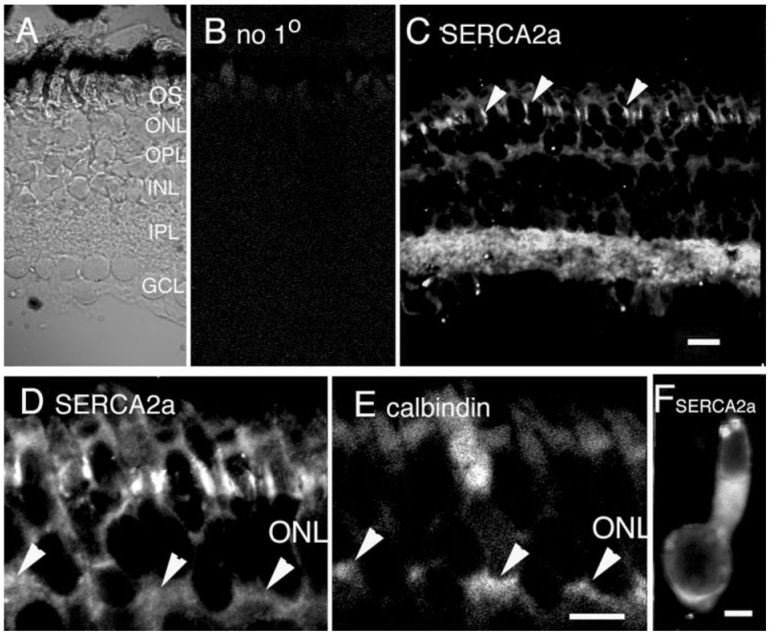


**Fig. 2.**

Localization of SERCA2a pumps in the salamander retina. **A:** Nomarski image of the salamander retina with annotated layers. **B:** Confocal micrograph of a vertical section through the salamander retina immunostained with secondary antibody alone. **C:** Confocal micrograph of the salamander retina immunostained with the SERCA2a antibody. The antibody labels photoreceptor inner segments in the ONL. Prominent signal in the IPL and moderate signals in the OPL and GCL are observed. Scale bar = 20 μm. **D:** Magnified view of SERCA2a staining in (C) focused on the ONL. The SERCA2a signal labeled cone photoreceptors, as shown by colocalization with calbindin in **E**. Calbindin labeled cone inner segments and synaptic terminals (arrowheads). Scale bar = 10 μm. **F:** Isolated cone photoreceptor. SERCA2a staining is seen in the subellipsoid region and the cell body. Scale bar = 5 μm.

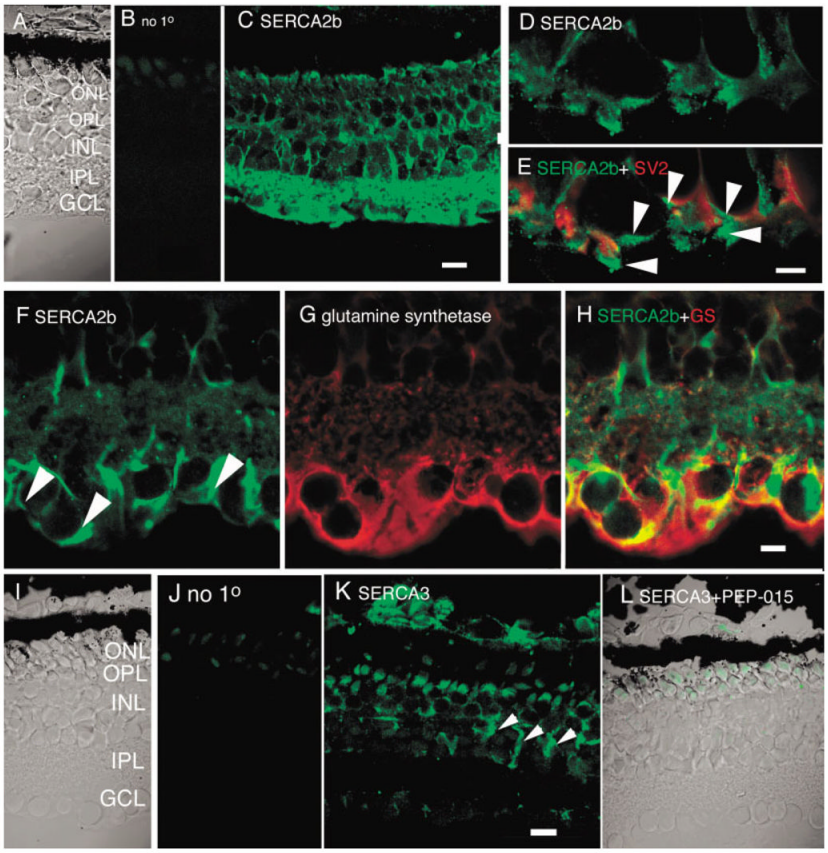


**Fig. 3.**

Immunostaining with (**A—H**) SERCA2b and (**I—L**) SERCA3 antibodies. C: SERCA2b is expressed in most retinal cells, including Müller glia processes and endfeet. Scale bar = 20 μm. D,E: Double-labeling of OPL with SERCA2b and synaptic marker SV2. SERCA2b is weakly expressed in photoreceptors; most of the SERCA2b signal occurs postsynaptically in the OPL. F—H: Colocalization with (F) SERCA2b and (G) glutamine synthetase. SERCA2b is prominently localized to endfeet and velate processes of Müller cells as well as to neuronal processes in the IPL. Scale bar = 10 μm. I—L: Immunostaining with the SERCA3 antibody. J: Little signal was detected in the absence of the primary antibody. Photoreceptor OSs were labeled nonspecifically. K: A diffuse SERCA3 signal was observed across all retinal layers, particularly in Müller cells (arrowheads). L: No SERCA3 signal was seen in the presence of the neutralizing peptide PEP-015. Scale bar = 20 μm.

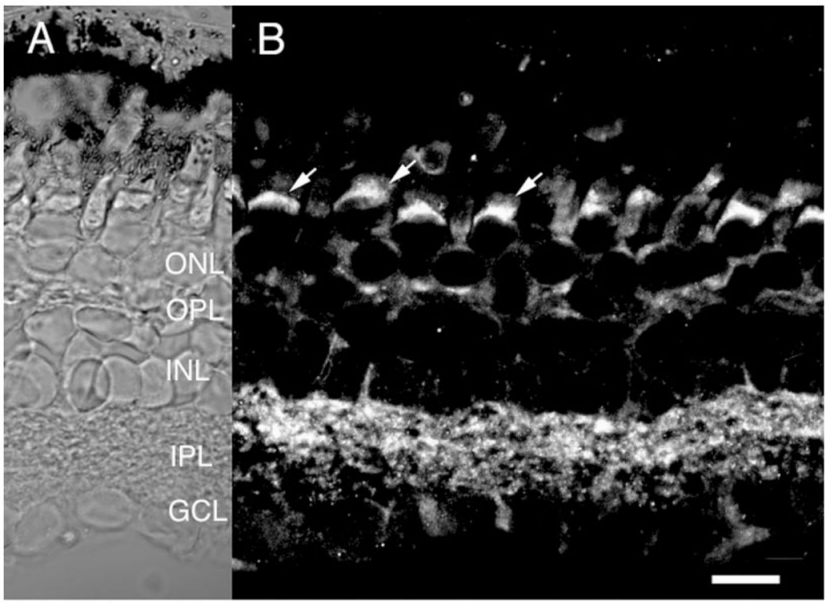


**Fig. 4.**

Salamander retina immunolabeled for RyR2. **A:** Nomarski image of the salamander retina. **B:** RyR2 immunofluorescence is found in the subellipsoid spaces (arrows) and cell bodies of photoreceptors and in both plexiform layers. Moderate labeling is seen presumed horizontal cell processes and in processes and endfeet of Müller glia (arrowheads). Scale bar = 20 μm.

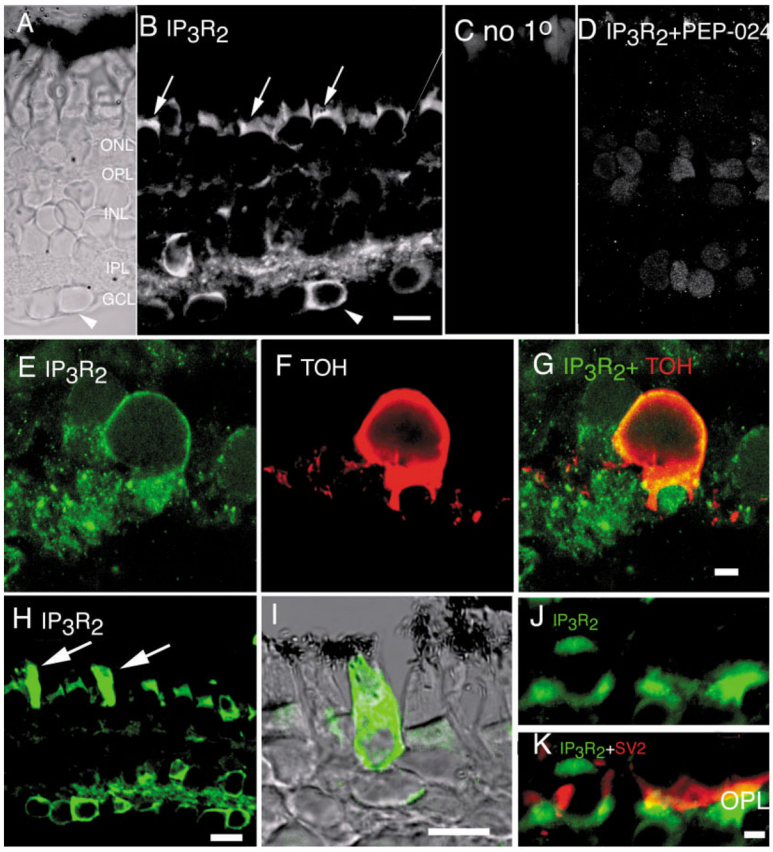


**Fig. 5.**

Salamander retina immunolabeled for $IP_3R2$. **A:** Nomarski image of the salamander retina. **B:** $IP_3R2$ immunofluorescence. **C:** Omission control. Subellipsoid spaces in photoreceptors are labeled (arrow) as well as horizontal and Müller cell processes in the OPL. A subpopulation of amacrine cell bodies in the proximal INL shows a prominent $IP_3R2$ signal, whereas Müller cell bodies in the central INL are moderately labeled. Some, but not all, cell bodies in the GCL exhibit a strong $IP_3R2$ signal; the arrowhead in A and B denotes one such cell. Note that its neighbor to the left is only weakly labeled. **D:** No $IP_3R2$-specific signal is seen when the antibody was coapplied together with the specific neutralizing peptide PEP-024. In the presence of PEP-024, diffuse labeling was often observed over cell somas in all layers. Scale bar = 20 μm. **E—G:** High-power fluorescence photomicrograph of the IPL double-labeled for $IP_3R2$ and TOH. Significant colocalization is seen in cell bodies of TOH-immunopositive neurons. The dendritic processes of TOH-positive neurons were typically did not express $IP_3R2$. Scale bar = 5 μm.

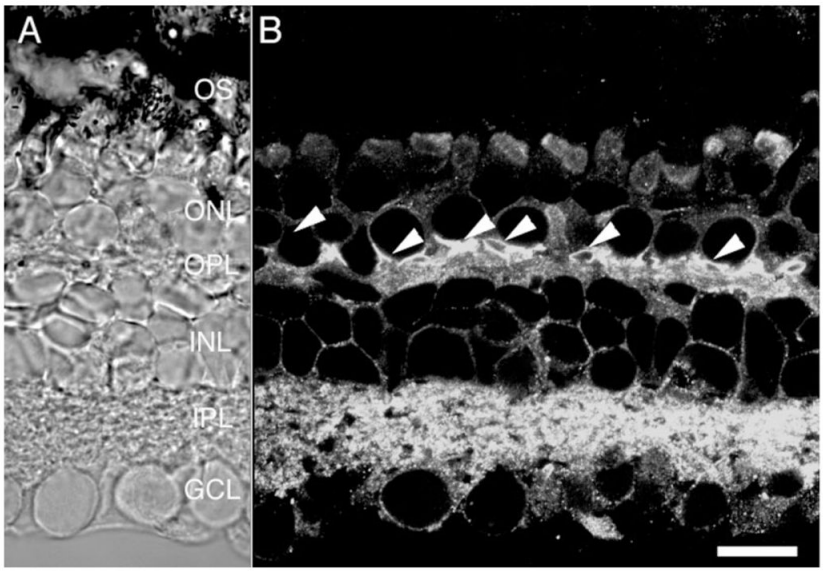


**Fig. 6.**

Salamander retina immunolabeled for PMCAs using the pan PMCA antibody 5F10. Synaptic terminals of photoreceptors are strongly labeled by 5F10 (arrowheads), as are amacrine and ganglion cell processes in the IPL. Cell bodies from photoreceptors, bipolar cells, amacrine cells, ganglion cells, and Müller cells are also labeled. Scale bar = 20 μm.

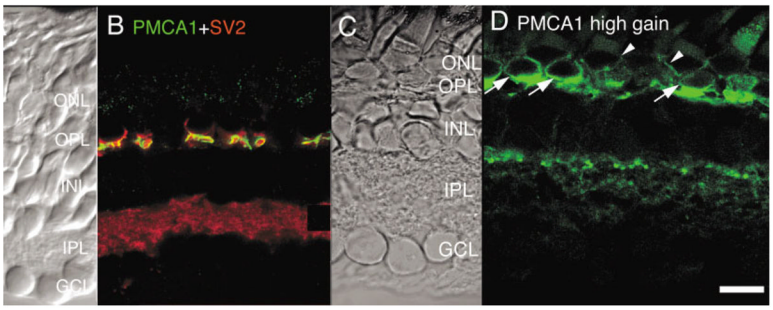


**Fig. 7.**

Salamander retina immunolabeled for PMCA1 and SV2. **A,C:** Nomarski images of the salamander retina. **B:** Double labeling for PMCA1 and SV2. PMCA1 (FITC) signal is localized to the OPL. PMCA1-imunopositive signals envelop the synaptic terminals of rod and cone photoreceptors labeled with the synaptic marker SV2. **D:** High gain PMCA1 immunofluorescence uncovers additional PMCA1 signal in cone (arrows) and rod (arrowheads) photoreceptor cell bodies and in processes in the OFF sublamina of the IPL. Scale bar = 20 μm.

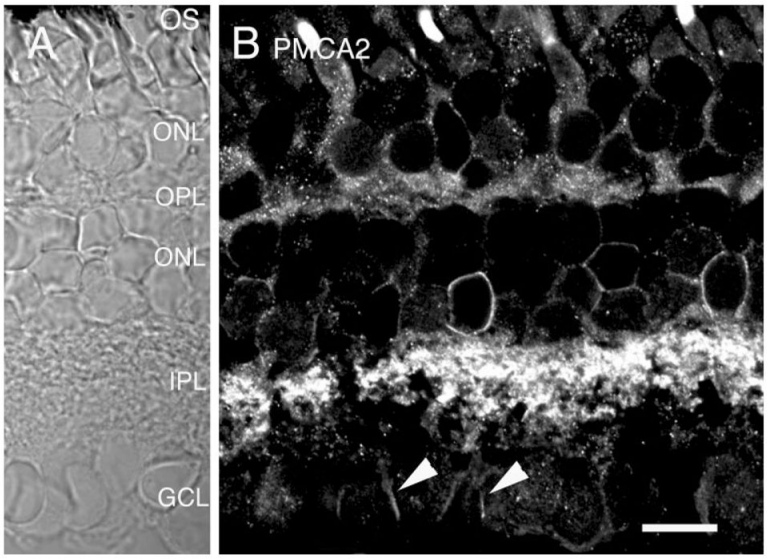


**Fig. 8.**

Salamander retina immunolabeled for PMCA2. **A:** Nomarski image of the salamander retina. **B:** PMCA2 immunofluorescence is found in all classes of retinal cells. Intense staining was often seen in ganglion cell bodies (arrowheads). Scale bar = 20 μm.

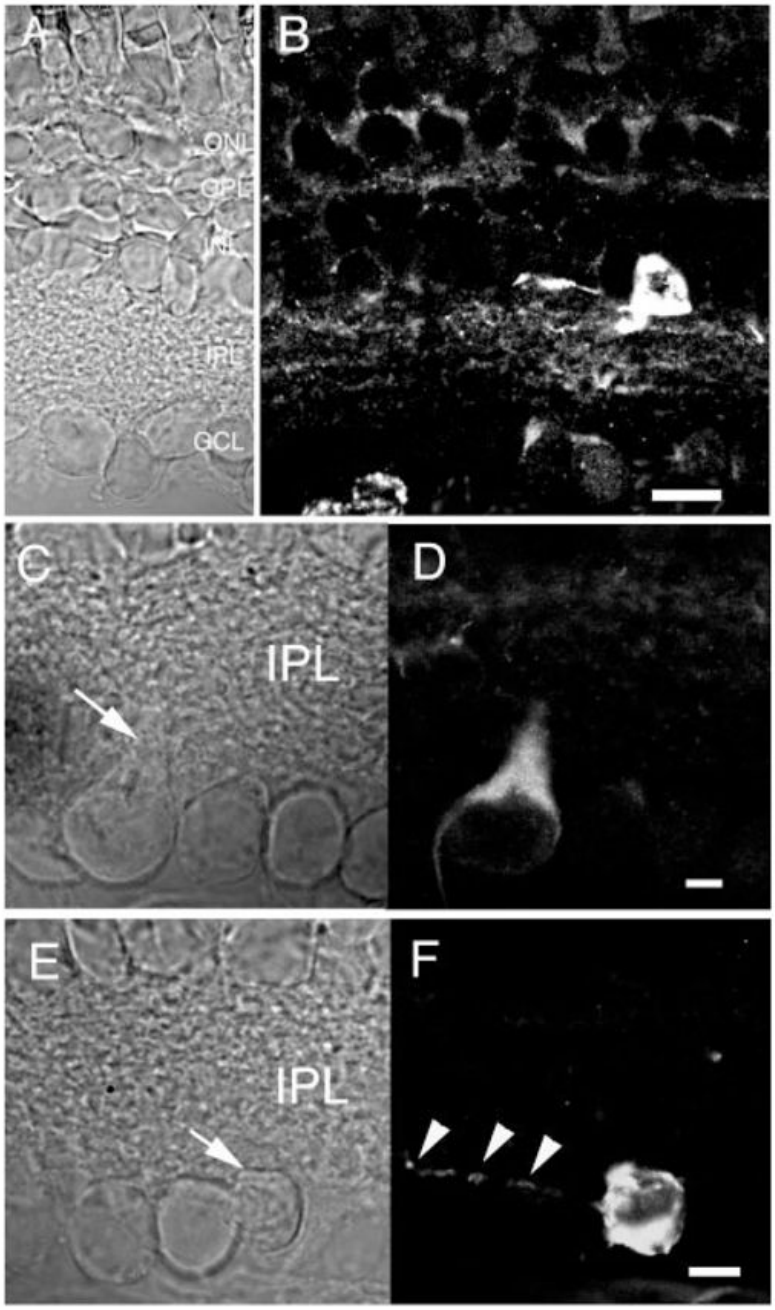


**Fig. 9.**

Salamander retina immunolabeled for PMCA3. **A,B:** The PMCA3 antibody labeled a sparse population of neurons in the proximal INL. The gain of the confocal system was increased to display the IPL processes of PMCA3-immunopositive cells. Scale bar = 20 μm. **C—F:** PMCA3 is expressed in a subset of ganglion layer neurons. C: Nomarski image of the GCL. D: The PMCA3 antibody labeled the primary dendrite and cell body of a subset of ganglion cells. E: Nomarski image of salamander GCL. F: PMCA3 antibody stained the cell body and dendritic processes of the ganglion cell marked with an arrow in E but not its neighboring cells in the GCL. Arrowheads mark the dendritic processes of the PMCA3-immunopositive cell. Scale bar for C–F = 10 μm.

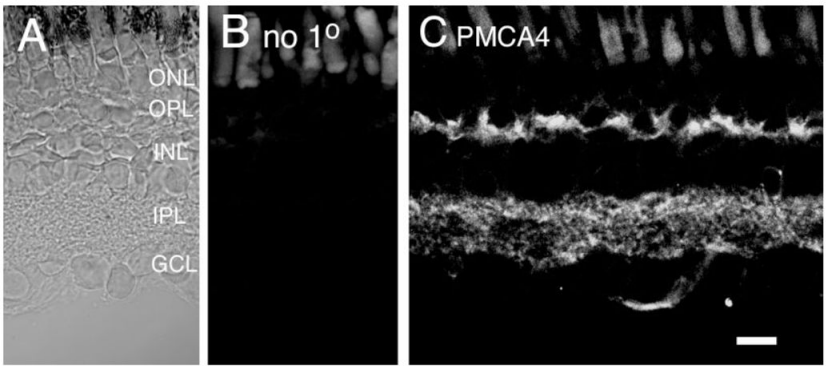


**Fig. 10.**
Salamander retina immunolabeled for PMCA4. **A:** Nomarski image of the salamander retina. **B:** Immunolabeling in the absence of the primary antibody. **C:** The PMCA4 antibody labeled photoreceptor terminals in the OPL and processes in the IPL. Scale bar = 20 μm.

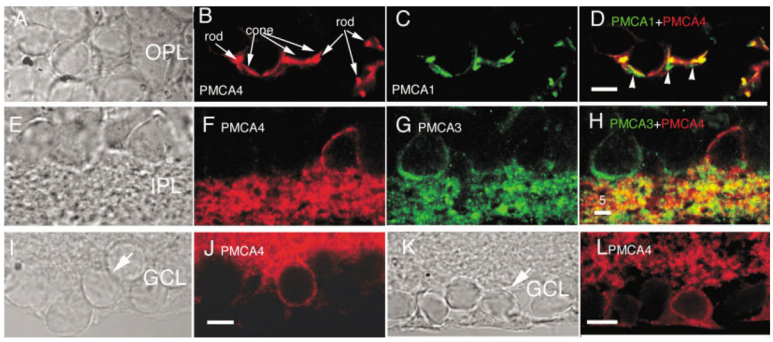


**Fig. 11.**

PMCA4 is expressed in photoreceptor terminals and in a subset of INL and GCL neurons. **A—D:** Colocalization of (B) PMCA4 and (C) PMCA1 in the OPL. PMCA4 and PMCA1 are expressed in synaptic terminals photoreceptors. PMCA isoforms 1 and 4 colocalize in most, but not all, synaptic processes. Scale bar = 10 μm. **E—H:** Selective expression of PMCA4 and PMCA3 isoforms. F: PMCA4 is expressed in a subset of amacrine neurons in the proximal INL. G: PMCA3 is expressed in different subset of amacrine cells. H: PMCA3 and PMCA4 do not colocalize in amacrine cells. Scale bar = 5 μm. **I—L:** PMCA4 is expressed in a subset of GCL neurons. Scale bar = 10 μm.

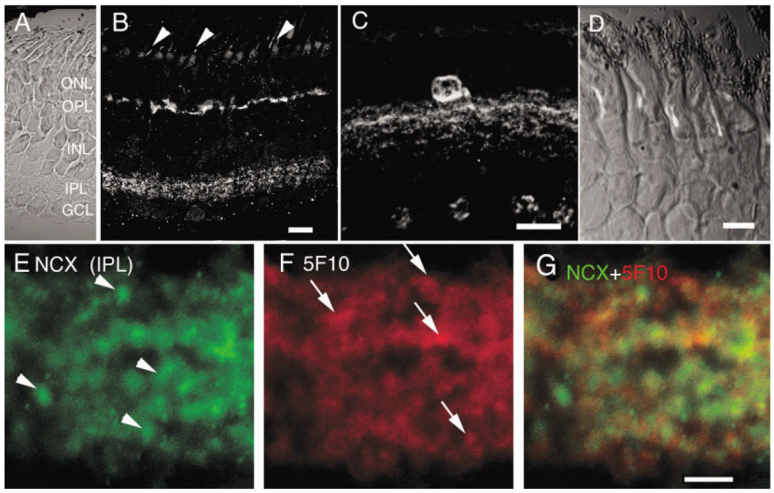


**Fig. 12.**

Salamander retina immunolabeled for the $Na^+/Ca^{2+}$ exchanger. **A:** Nomarski image of the salamander retina. **B:** NCX immunoreactivity is found in the IPL as well as cell processes in the proximal OPL. A compartment within the OS corresponding to the axonemal region was also labeled by the NCX antibody (arrowheads). Scale bar = 20 μm. **C:** A subclass of amacrine cell bodies with dendritic processes ramifying in the distal IPL was found to be strongly NCX-immunoreactive. Scale bar = 20 μm. **D:** A higher magnification view of the ONL and OSs. Scale bar = 10 μm. **E—G:** A magnified view of salamander IPL, double-labeled for NCX and PMCA (5F10). Scale bar = 5 μm.

**TABLE 1**

Antibodies Used

| Antigen | Ab source | Dilution | Designation | Source |
|---|---|---|---|---|
| PMCA1–3 | rabbit | 1 to 300 or 1 to 500 | NR1–3 | J.Penniston. Swant, ABR |
| PMCA4 | mouse | 1 to 100 | JA9 | J.Penniston. ABR |
| PMCA4 | rabbit | 1 to 100 | PMCA4 | Swant |
| pan PMCA | mouse | 1 to 100 | 5F10 | Sigma, ABR |
| Na/Ca exchanger | rabbit | 1 to 100 or 1 to 500 | p11–13 | Swant |
| SERCA1 | rabbit | 1 to 100 | CaF2-5D2 | Dev. Studies Hybridoma Bank |
| SERCA2 | mouse | 1 to 500 | MA3–919 | ABR |
| SERCA2a | rabbit | 1 to 100 or 1 to 500 | | F. Wuytack |
| SERCA2b | rabbit | 1 to 300 | | F. Wuytack |
| SERCA3 | rabbit | 1 to 100 | N89 | Sigma |
| pan RyR | rabbit | 1 to 100 | | F.A. Lai |
| RyR1 | rabbit | 1 to 100 | | Dev. Studies Hybridoma Bank |
| RyR2 | rabbit | 1 to 100 | #33, #1033 | F.A. Lai |
| IP3R1 | rabbit | 1 to 100 | AB5882 | Chemicon |
| IP3R2 | rabbit | 1 to 500 | PA1–904 | ABR |
| IP3R3 | mouse | 1 to 100 | #610312 | Transduction Labs |
| SV2 | mouse | 1 to 100 | | Dev. Studies Hybridoma Bank |
| tyrosine hydroxylase | mouse | 1 to 500 | MAB318 | Chemicon |

*J Comp Neurol*. Author manuscript; available in PMC 2008 November 5.